DOI: http://dx.doi.org/10.32571/ijct.1004065 E-ISSN: 2602-277X

International Journal of Chemistry and Technology

http://dergipark.org.tr/ijct

Research Article

Structural and spectral properties of 4-(4-(1-(4-Hydroxyphenyl)-1-phenylethyl)phenoxy)phthalonitrile: Analysis by TD-DFT method, ADME analysis and docking studies

Kenan ALTUN[1], Ümit YILDIKO[1], Aslıhan Aycan TANRIVERDİ[2,*], İsmail ÇAKMAK[2]

[1] *Engineering and Architecture Faculty, Department of Bioengineering, Kafkas University, Kars, 36100, Turkey*

[2] *Faculty of Arts and Sciences. Department of Chemistry, Kafkas University, Kars, 36100, Turkey*

Received: 3 October 2021; Revised: 3 December 2021; Accepted: 8 December 2021

*Corresponding author e-mail: t.aslihanaycan@gmail.com

Citation: Altun, K.; Yıldıko, Ü.; Tanrıverdi, A. A.; Çakmak, İ. *Int. J. Chem. Technol.* **2021**, 5 (2), 147-155.

ABSTRACT

Since phthalonitrile compounds have become popular lately, the focus has been on the idea that these compounds should be investigated. A unique phthalonitrile compound, 4-(4-(1-(4-hydroxyphenyl)-1-phenylethyl)phenoxy)phthalonitrile (coded as PN) was selected and molecular modeling studies were carried out on this compound to be brought to the literature. First, time-dependent density functional theory (TD-DFT) calculations (Geometry optimization, HOMO-LUMO, dipole moment calculations, MEPS maps, Mulliken atomic charges, and NBO analysis) were performed for PN. In addition, in this section, absorption, distribution, metabolism, excretion, and toxicity (ADMET) analysis for the compound belonging to the phthalonitrile group was performed and the color regions were presented separately. Finally, molecular docking studies were performed for a compound separately with three different enzymes (AChE, BChE, α-GLY), and docking scores and receptor models were presented.

Keywords: Phthalonitrile, TD-DFT, ADMET, molecular docking.

4-(4-(1-(4-Hidroksifenil)-1-feniletil) fenoksi) ftalonitril'in yapısal ve spektral özellikleri: TD-DFT metodu ile analiz, ADME analizi ve doking çalışmaları

ÖZ

Ftalonitril bileşikleri son zamanlarda popüler hale geldiğinden, bu bileşiklerin araştırılması gerektiği fikri üzerinde durulmuştur. Eşsiz bir ftalonitril bileşiği olan, 4-(4-(1-(4-hidroksifenil)-1-feniletil)fenoksi)ftalonitril (PN olarak kodlanmıştır) seçilmiş ve literatüre kazandırılmak üzere bu bileşik üzerinde moleküler modelleme çalışmaları yapılmıştır. İlk olarak, PN için zamana bağlı yoğunluk fonksiyonel teorisi (TD-DFT) hesaplamaları (Geometri optimizasyonu, HOMO-LUMO, dipol moment hesaplamaları, MEPS haritaları, Mulliken atom yükleri ve NBO analizi) yapılmıştır. Ayrıca bu bölümde ftalonitril grubu bileşiğe ait absorpsiyon, dağılım, metabolizma, atılım ve toksisite (ADMET) analizleri yapılmış ve renk bölgeleri ayrı ayrı sunulmuştur. Son olarak, bir bileşik için ayrı ayrı üç farklı enzim (AChE, BChE, α-GLY) ile moleküler doking çalışmaları yapılmış ve doking skorları ve reseptör modelleri sunulmuştur.

Anahtar Kelimeler: Ftalonitril, TD-DFT, ADMET, Moleküler doking.

1. INTRODUCTION

In the last few years, phthalonitriles (PNs) have remarked many attention for their extraordinary features. The enhanced heat resistance of phthalonitriles also shows other highly attractive performances such as an outstanding flame resistance, well mechanical properties at high temperature, low water uptake, outstanding corrosion resistance, and developed UV protection behavior.[1] However, PN materials have brittleness property. Brittleness, an inherent property of PNs, results from the hardness of monomeric vanguards and the high degree of crosslinking of their cured versions.[2] Additionally, normal PN monomers require higher curing temperatures and a longer time to attain completely cured systems. Although the inset of multi

DOI: http://dx.doi.org/10.32571/ijct.1004065 E-ISSN: 2602-277X

curing catalysts was contrived to enhance curing attitude to a significant rating, curing temperatures and times did higher than those of other high-performance thermosets.[3,4] The afore mentioned PN deficiencies were examined by researchers and many solutions were recommended. Introduced functionalities involved imide, alkene, bismaleimide, alkyl, benzoxazine, benzimidazole, novolac, and the like. Functionality election is often driven by targeted features. Other functions can ensure both improvements.[5] When the PN monomer does not encounter all the necessaries for a particular application, forming blends and copolymers with another PN compound is the first choice before careful blending with other types of monomers.[6] The diversity of PN monomers present, involving typical, functional, and self-catalyzing PN monomers and oligomers with different features, may direction some of the limitations of a single PN monomer.[7]

Methods for predicting the 3-d structure of a protein generally fall into three categories: ab initio or de novo modeling, threading, and homology or comparative modeling. Ab initio modeling uses a combination of statistical analysis and physics-based energy function to estimate the natural multiple of a delivered sequence.[8] Ab initio modeling is favoured for estimating the structure of a sequence when no convenient template is found or when the query is common to use a particular fold than the envisaged template despite sequence similarity.[9] Various ab initio algorithms exercise statistical information, secondary structure, and part assemblage for folding forecast. Also common to all algorithms is the simplistic presentment of the protein to keep the forecast problem traceable. Reference is made to the reader for more information on the particular ab initio estimation methods.[10,11]

In this study, molecular modeling studies of a selected unique PN compound were carried out. TD-DFT studies were carried out to have information about the energy properties, electrical properties, and nonlinear optical properties of the compound. In addition, ADME analysis was carried out to investigate the ADMET properties of the compound. Finally, molecular docking studies have been carried out successfully to determine whether the PN compound will be compatible with the drug design phenomenon.

2. MATERIALS AND METHODS

2.1. Computer calculations

The PN molecule was first drawn in ChemBioDraw for TD-DFT calculations in the gaussian 09 program and minimized by the SYBL2 (mol2) method with the Chem3D program. Similarly, the drawn molecules were converted to 3D MOL2 files in Chem3D and transferred to GaussView 6.0. TD-DFT study[12] was calculated on 6-311G basis set in B3LYP and LanL2DZ method and images of each calculation[13] (Geometry optimization, HOMO and LUMO analysis, Mulliken atomic charges and dipole moment, MEP analysis) were taken. Molecular docking was provided to investigate the exact binding site and binding mechanism of ligand-protein interactions. Schrödinger's Maestro Molecular Modeling platform (version 11.8).[14] Online servers such as SwissADME (http://www.swissadme.ch/index.php) were used for ADME analysis.[15] The LLC model was applied in the molecular docking approach. Crystal structures of human asetilkolinesteraz (AChE) (PDB ID: 4M0E), butirilkolinesteraz (BChE) (PDB ID: 6SAM) ve alfa-glukosidaz (α-GLY) (PDB ID: 3A4A) enzymes were downloaded. All compounds were equipped as for that former studies with the Ligprep module. Ligand-protein docking studies were carried out with the glide docking module. The highest binding energies and binding conformations between enzymes and ligands were estimated.[16] The lowest energy positions show the highest binding affinities. Molecular docking study were visualized with Discovery Studio 2016 client (Visualizer 2005).

3. RESULTS AND DISCUSSION

The molecule belonging to the phthalonitrile group was first drawn in ChemBioDraw for theoretical calculations in the Gaussian 09 program and applied by the "PDB" format method with the Chem3D program. Applied molecules were given to the Gaussian 09 program and ab initio calculations were done for this structure.

3.1. TD-DFT Studies

3.1.1. Geometry optimization of PN compound

The theoretically calculated values of some phthalonitrile compounds can give an idea about the geometry of molecular changes.[17,18] The optimized basic structure and total energy conversion of PN are given in Figure 1.

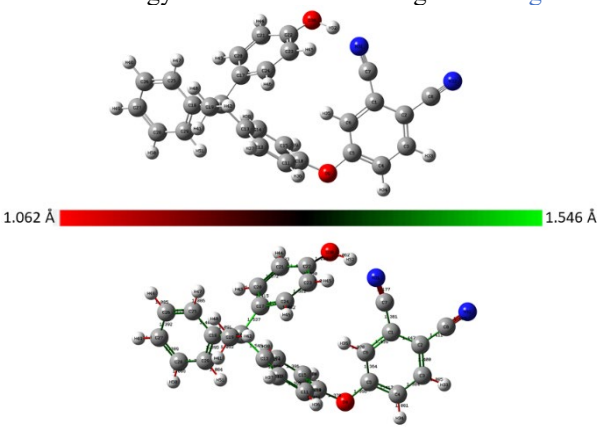

Figure 1. Optimized structure for PN using the TD-DFT method and the R3PW91 / TD-FC and RB3LYP/6-311G (d, p) basis set.

DOI: http://dx.doi.org/10.32571/ijct.1004065 E-ISSN: 2602-277X

The optimized bond length parameters of the molecule calculated with the TD-FC basis set of R3PW91 and the 6-311G (d, p) basis set of RB3LYP in the PN TD-DFT method are shown in Figure 1 and listed in Table 1. There is very little difference between the R3PW91 and RB3LYP values. This means that the structure has minimum potential energy. A comparison of optimized two basis set of PN was studied. All bond lengths and bond angles in phenyl rings are within the normal range. The C-C bond distances for R3PW91 are 1.361-1.545 Å, and the C-O bond distances for RB3LYP are 1.363-1.555 Å and 1.288-1.405 Å for the oxygen atom between the two phenyl rings. The C-H lengths in the aromatic ring are 1.076 - 1.091 Å. All C-C-C angles are between 112° and 123°. The C-C-H angle in the compound is 112° - 121°, C-C-O 115° -123°, and O-C-H 112-113°.

Table 1. The theoretically obtained bond lengths (Å), bond angles (°), and dihedral angles (°) of the molecule for PN.

Bond lengths (Å)			Bond Angles (°)		
Atom Groups	**R3PW91**	**RB3LYP**	**Atom Groups**	**R3PW91**	**RB3LYP**
C1-C2	1.44698	1.45150	C1-C2-C8	121.41592	121.39628
C1-C6	1.43875	1.44267	C1-C2-C3	118.48142	118.47263
C2-C3	1.39996	1.40259	C2-C8-N32	179.70130	179.64954
C2-C8	1.41060	1.41301	C1-C7-N31	172.70007	172.58947
C8-N32	1.16159	1.16117	C2-C3-H33	117.85024	117.85481
C3-H33	1.08452	1.08370	C1-C6-H35	117.99770	117.86282
C3-C4	1.38446	1.38648	C14-C15-H39	121.02220	120.94766
C4-H34	1.08135	1.08041	C6-C5-O9	122.93404	122.97260
C4-C5	1.41656	1.41929	C5-C4-H34	119.83494	119.82089
C5-C6	1.36368	1.36422	C5-O9-C10	115.62031	116.03688
C6-H35	1.07815	1.07656	C3-C4-C5	118.35084	118.31576
C5-O9	1.39623	1.40504	C10-C11-H36	119.07370	119.07862
C1-C7	1.38134	1.38401	C10-C11-C12	119.90458	119.94643
C7-N31	1.17695	1.17685	C10-C15-H39	119.21409	119.21882
O9-C10	1.36993	1.37458	C11-C12-C13	120.99433	121.05933
C10-C11	1.38872	1.39056	C12-C13-C16	122.38367	122.36303
C11-H36	1.08383	1.08296	C12-C13-C14	117.80020	117.64938
C10-C15	1.39258	1.39444	C13-C14-H38	119.74895	119.85308
C15-H39	1.08375	1.08282	C13-C16-C18	114.03440	114.08505
C14-C15	1.38572	1.38782	C13-C16-C19	112.51612	112.44122
C14-C13	1.40329	1.40569	C16-C19-H42	113.40299	113.42896
C14-H38	1.08491	1.08351	H40-C19-H41	107.79547	107.81048
Dihedral Angles (°)			**Dihedral Angles (°)**		
Atom Groups	**R3PW91**	**RB3LYP**	**Atom Groups**	**R3PW91**	**RB3LYP**
C1-C2-C3-C4	0.46233	0.42841	C23-C22-O30-H52	17.82858	18.19702
C2-C1-C7-N31	179.01002	178.23777	H46-C24-C23-H45	0.04831	0.28348
C3-C4-C5-09	179.66344	179.70866	C12-C13-C16-C18	133.08575	133.14003
H36-C11-C10-O9	4.56578	4.79244	H48-C26-C27-H49	0.29434	0.30255

3.1.2. Frontier molecular orbitals (HOMO-LUMO) and dipole moment calculations of the PN compound

The main electrical parameters regarding orbitals in a molecule are the highest occupied molecular orbital (HOMO) and lowest unoccupied molecular orbital (LUMO) and energy vacancies. HOMOs are the outermost (highest energy) orbital electrons that can act as electron donors. The LUMO is the innermost (lowest energy) orbital that has enough space to accept electrons and can act as an electron acceptor. The HOMO and LUMO orbitals determine the interaction of the molecule with other sort.[19] The orbital representation of HOMO and LUMO for density PN is shown in Figure 2. Calculated using the TD-DFT method from E_{HOMO} - 5.3480 eV - E_{LUMO} -3.3726 eV for the TD-FC basis set of R3PW91 and E_{HOMO} - 5.3172 eV - E_{LUMO} - 3.2913 eV for the 6-311G (d, p) basis set of RB3LYP (Figure 2). The HOMO and LUMO orbitals determine how the molecule interacts with other species. It also helps characterize the bandgap, chemical reactivity, and kinetic stability. A small border indicates the electronegativity, hardness, polarization, and other reactivity indices of a molecule with an orbital gap. Table 2 shows the chemical reactivity indices.

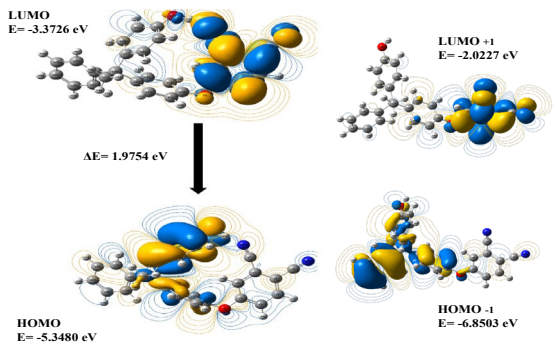

Figure 2. HOMO-LUMO energy maps and bandgap for PN using the TD-DFT method and the R3PW91/TD-FC basis set.

DOI: http://dx.doi.org/10.32571/ijct.1004065 E-ISSN: 2602-277X

The dipole moment is an important property of the energy associated with the applied electric field of molecule.[20] The dipole moment consists of intermolecular interactions involving Van der Waals type dipole-dipole forces and generates strong intermolecular attraction. Table 3 shows the calculated parameters, electronic dipole moment, and total dipole moment.

Table 2. Comparison of HOMO, LUMO, energy gaps (D), and PN-related (au) molecular properties for PN.

Molecular Energy	R3PW91	RB3LYP
E_{LUMO}	-3.3726	- 3.2913
E_{HOMO}	-5.3480	- 5.3172
E_{LUMO+1}	-2.0227	- 1.9617
E_{HOMO-1}	-6.8503	- 5.3172
Energy Gap (Δ) $\lvert E_{HOMO}- E_{LUMO}\rvert$	1.9754	2.0259
Ionization Potential ($I = -E_{HOMO}$)	5.3480	5.3172
Electron Affinity ($A = -E_{LUMO}$)	3.3726	3.2913
Chemical Hardness ($\eta = (I - A)/2$)	0.9877	1,0129
Global Softness ($s = 1/2\ \eta$)	0.4938	0,5064
Chemical Potential ($\mu = -(I + A)/2$)	-4.3603	-4,3042
Electronegativity ($\chi = (I + A)/2$)	4.3603	4,3042
Global Electrophilicity ($\omega = \mu^2/2\ \eta$)	9,6245	9,1453

Table 3. For PN, dipole moments (Debye), (au) polarizability, β components and value of β tot phthalonitrile are calculated by TD-DFT method for R3PW91/TD-FC and RB3LYP /6-311G (d, p) basis set.

Parameter	R3PW91	RB3LYP	Parameter	R3PW91	RB3LYP
μ_x	-0.6581	-0.7534	β_{XXX}	-249.4849	-250.2618
μ_y	-6.0908	-6.0036	β_{XXY}	-141.4082	-142.4993
μ_z	0.5071	0.5107	β_{XYY}	-5.0885	-6.3562
$\mu_{(D)}$	6.1472	6.0722	β_{YYY}	-61.7956	-59.9208
α_{xx}	-192.7117	-195.1953	β_{XXZ}	-32.4278	-29.7575
α_{yy}	-195.0605	-196.8636	β_{XYZ}	10.9778	11.3327
α_{zz}	-178.1407	-179.7363	β_{YYZ}	-1.9491	-1.5071
α_{XY}	-25.0475	-24.9492	β_{XZZ}	-5.1822	-3.1047
α_{XZ}	3.0576	3.0537	β_{YZZ}	-12.0244	-11.4329
α_{YZ}	2.7554	2.8848	β_{ZZZ}	7.9632	6.9515
α(au)	-188.6376	-190,5984	β(esu)	$3.3x10^{-30}$	$3.0x10^{-34}$

3.1.3. Molecular electrostatic potential surface (MEPS) maps of PN

The molecular electrostatic potential surface MEPS shows the size, shape, and electrostatic potential values of the molecule and is plotted for the phthalonitrile molecule. MEPS mapping is very beneficial in investigating the physicochemical properties of molecular structure.[21] The green color indicates neutral electrostatic potential. Here, MEPS maps were mapped for PN as shown in Figure 3. In the case of phthalonitrile, the MEPS map shows negative potential regions around the nitrogen atoms, characterized by red color. It shows

DOI: http://dx.doi.org/10.32571/ijct.1004065 E-ISSN: 2602-277X

an almost neutral potential as most of the aromatic ring region is represented by green.

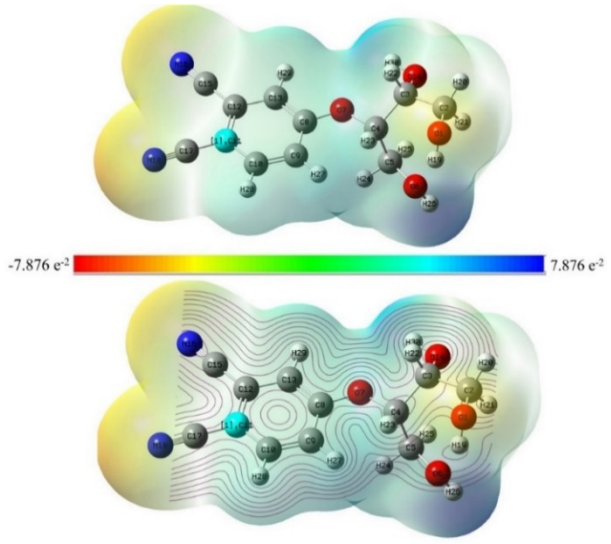

Figure 3. MEPS mappings for PN.

3.1.4. Mulliken atomic charges of PN

The calculation of Mulliken atomic charges plays an important role in applying quantum chemical calculations. Mulliken atom was calculated for PN on the basis set of R3PW91/TD-FC and RB3LYP/6-311G (d, p) by the TD-DFT method. The graph comparing the Mulliken atomic charges for PN is presented in Figure 4. The data obtained from the calculations are presented in Figure 5 and Table 4. The distribution of Mulliken charge is that the oxygen atom attached to the aromatic ring is O1 (-0.403) - (-0.500), O6 (-0.435) - (-0.539), O7 (-0.381) - (-0.359). It was observed that some C atoms were positive and some were negative.

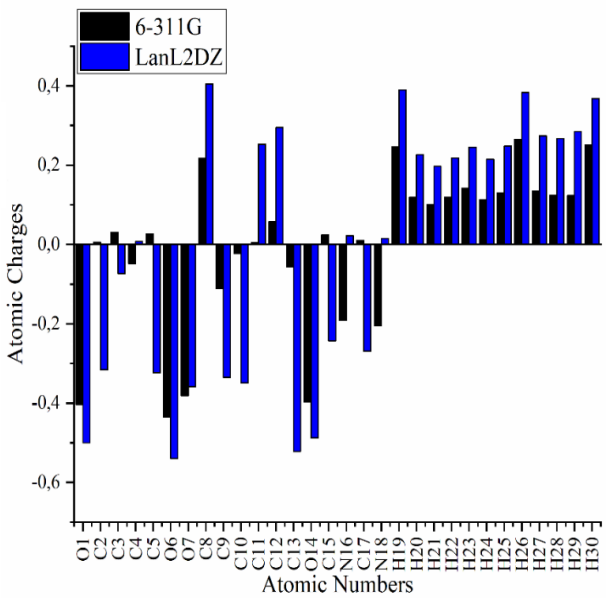

Figure 4. Comparison of Mulliken atomic charges for PN.

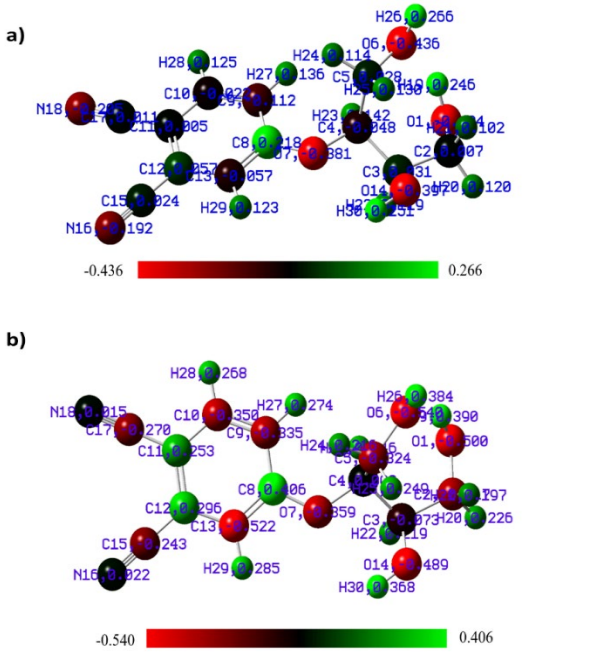

Figure 5. The Mulliken atomic charges of a) R3PW91 / TD-FC and b) RB3LYP/ 6-311G (d, p) basis set by TD-DFT method for PN.

3.1.5. NBO analysis of PN

NBO analysis provides research on the most accurate Lewis structure of the molecule, detailed electron density of all orbitals, NBO method is an evaluation of full and empty orbital interactions that provides information about both intermolecular and intermolecular interactions. A quadratic Fock matrix was constructed to evaluate the donor-receiver interactions in the NBO analysis of our compound. The result of the interaction is a loss of occupancy from a localized NBO of the idealized Lewis structure to an empty non-Lewis orbital. For each transmitter (i) and receiver (j), the stabilization energy associated with the displacement of i → j is estimated as E (2). NBO analysis was performed to explain charge transfer or charge displacement due to intramolecular interaction between bonds. These results are measurements of delocalization and hyperconjugation, the results analyzed for PN are given in Table 5.

Intramolecular interactions are observed as an increase in electron density (ED) in the antibody orbitals weakening the respective bonds (C - O), The electron density of the conjugated substituted bond (1.9938 au) indicates a strong dislocation, the occupancy rate of Σ bonds is higher than that of σ* bonds. high, which provides greater localization. The intramolecular hyper conjugative interaction of the distribution to π (C8-C9) π electrons in the ring leads to stabilization of a portion of the ring, as seen in Table 5. π* (C10-C11) and anti-Ring * (C12-C13) lead to 25.61-18.56 kcal/mol stabilization. These values increased conjugation leading to strong localization.

DOI: http://dx.doi.org/10.32571/ijct.1004065 E-ISSN: 2602-277X

3.2. ADME analysis of PN

Currently, ADME studies in drug manufacturing are used to select the most promising compounds and to minimize the risk of late-stage drug wear. With these studies, a balance between pharmacodynamic and pharmacokinetic properties can be determined as preliminary information.[22] Here, many parameters such as molecular properties, drug solubility S, cell permeability, HIA, polar surface area PSA, and drug similarity score were investigated by virtual scanning methods on small molecules. An existing oral drug selected according to Lipinski's rule of 5 should have a molecular weight and LogP of no more than 500 and 5, respectively, less than 10 hydrogen bond acceptors, and less than 5 hydrogen bond donors.

Online servers such as SwissADME (http://www.swissadme.ch/index.php) were used. The results in Table 6 show that the compounds are coherent with MA 276.25-416.47 g/mol (<500), LogP values 1.54 -4.99 (<5), and acceptor hydrogen bond (AHB) 4-6 (<10) according to Lipinski's rule. Topological PSA values are between 77.04 - 99.89 <140, A2 ABS is between 74.54-82.42% (Figure 6).

Table 5. Selected NBO results for PN were calculated for the R3PW91/TD-FC baseset by the TD-DFT method.

NBO(i)	Type	ED/e	NBO(j)	Type	ED//e	E(2)[a] (Kcal/mol)	E (j)-E(i)[b] (a,u,)	F (i, j)[c] (a,u)
O1-C2	σ	1.99381	C3-O14	σ*	0.04747	1.31	1.11	0.034
O1-H19	σ	1.98833	C2-H20	σ*	0.02047	1.55	1.12	0.037
			C2-H21	σ*	0.02569	0.96	1.10	0.029
C2-C3	σ	1.97792	C3-C4	σ*	0.04747	0.72	0.96	0.024
			C3-H22	σ*	0.03218	0.55	1.01	0.021
			C4-O7	σ*	0.03349	2.51	0.86	0.042
			O14-H30	σ*	0.00765	1.73	1.03	0.038
C5-H24	σ	1.98516	C3-C4	σ*	0.04747	3.07	0.88	0.047
			C4-O7	σ*	0.03349	1.36	0.78	0.029
			C4-H23	σ*	0.02617	2.56	0.93	0.044
O6-H26	σ	1.98875	C4-C5	σ*	0.03155	2.10	1.08	0.043
O7-C8	σ	1.99010	C12-C13	σ*	0.02208	1.01	1.70	0.037
C8-C9	σ	1.97976	C8-C13	σ*	0.02054	4.03	1.24	0.063
			C9-C10	σ*	0.01337	2.82	1.27	0.054
			C10-H28	σ*	0.01201	2.51	1.15	0.048
	π	1.59934	C10-C11	π*	0.38304	25.61	0.28	0.076
			C12-C13	π *	0.37067	18.56	0.27	0.064
C15-N16	σ	1.99344	C12-C15	σ*	0.03019	10.02	1.58	0.113
C17-N18	σ	1.99390	C11-C17	σ*	0.03091	9.28	1.57	0.108
			C10-C11	σ*	0.02334	3.20	0.85	0.047
			C11-C12	σ*	0.04047	3.89	0.79	0.050

Table 6. Physicochemical and lipophilicity of the most active compounds.

Code	Lipophilicity consensus log P	Physico-chemical properties								
		MA[a] g/mol	Heavy atoms	Aromatic heavy atoms	Rot. bond	H-bond acc.	H-bond don.	MR[b]	TPYA[c] (A^2)	% ABS[d]
PN	4.99	416.47	32	24	5	4	1	123.04	77.04	82.42

[a]**MA**, molecular weight; [b]**MR**, molar refractivity; [c]**TPYA**, topological polar surface area; [d]**ABS%:** absorption percentage (ABS% = 109 − [0.345 × TPYA]; [e]Quinic acid; [f]Quercitrin; [g]Miquelianin).

DOI: http://dx.doi.org/10.32571/ijct.1004065 E-ISSN: 2602-277X

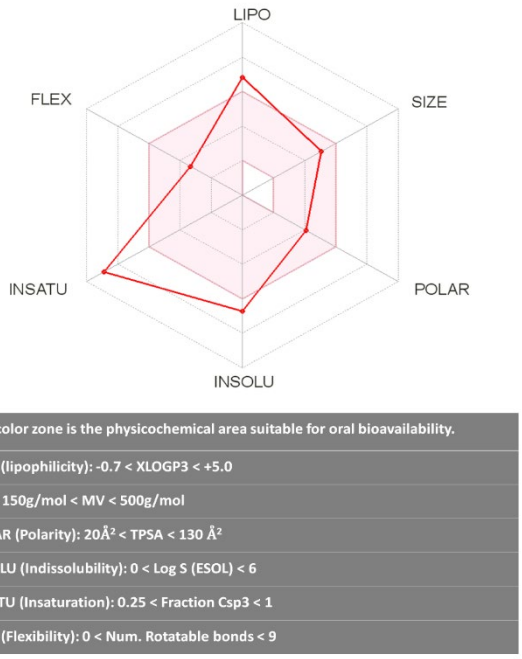

Figure 6. Color regions and physicochemical parameters of PN.

3.3. Molecular docking studies of PN

Molecular docking is useful for investigating the ligand-receptor binding mechanism and for learning about the interaction of binding modes at the molecular level.[23,24] Molecular docking was performed to identify the selected binding sites of ligands with the receptor and to largely approve the experimental observations. In this study, which consisted of one compound and three enzyme sets, three good docking scores were found (Table 7). These ligands were docked to the catalytic active site of the enzyme and the docking results were examined on the basis of binding affinity and interaction mode. However, in terms of molecular structure, the best binding affinity score was seen in BchE enzyme.

Table 7. The best binding affinity scores (kcal/mol) of compounds in the catalytic sites of enzymes.

Phenolic Compound	Docking Score		
	AChE (PDB: 4M0E)	BChE (PDB:6SAM)	α-GLY (PDB:3A4A)
PN	-8.01	-8.332	-5.209

The similarity of the protein structure to the natural ligand increases this value because it is structural. The dynamics of the protein plays an important role in how proteins must interact with a number of derivatives to form complexes that can enhance or limit their biological functions. After choosing the best pose in the whole ligand-enzyme docking study, the binding modes were analyzed to comprehend the inhibition mechanisms. Figure 7 shows the 3D and 2D interaction as a result of the PN-AChE docking study. The affinity score for binding affinity with PN-AChE was calculated as -8.01 kcal/mol. Here, HOH-869 (1.76 Å) hydrogen-bonded water hydrogen bond to phenol in the bonding mechanism, VAL-340 (3.07 Å) bonded with hydrogen-bonded to phenol, Conventional Hydrogen Bond with PHE-295 (2.01 Å) bound to the first Nitrogen of phthalonitrile and (2.81 Å) bound to the second Nitrogen of TYR-337 phthalonitrile, VAL-294 (3.03 Å) carbon-hydrogen bond attached to the first Nitrogen of phthalonitrile, TRP-286 (4.31 Å) and TYR-341 (4.19 Å) Pi-Pi stacking attached to the center of the phthalonitrile benzene ring, LEU-76 (5.44 Å) Pi-Alkyl bonded to the center of the benzene ring, TYR-124 (5.66 Å) are examples of Pi-Pi T-shaped bonded to the center of the benzene ring and other interactions are as in Figure 7.

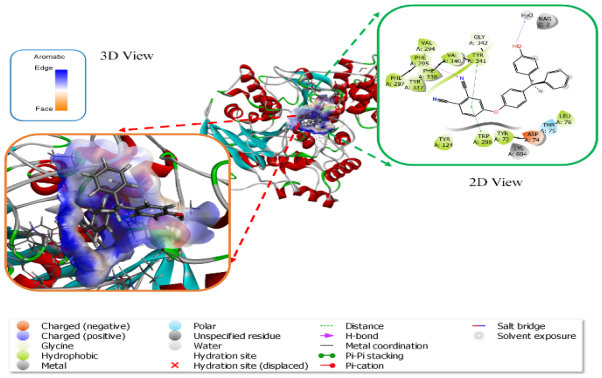

Figure 7. 3D view of the aromatic surface on the receptor and 2D view of PN-AChE enzyme interactions.

Figure 8 shows the 3D and 2D interaction as a result of the PN-BChE docking study. In binding affinity with PN-BChE, the highest affinity score was calculated as -8.332 kcal/mol. Here, in the bonding mechanism, ALA-328 (2.72 Å) and ASN-289 (2.14 Å) hydrogen-bonded conventional hydrogen bond to phenol, PHE-329 (4.36 Å) benzene ring bonded to center Pi-Pi stacking, and also (4.36 Å) Pi- Pi T-shaped, TYR-332 (2.80 Å) Pi-donor hydrogen bond to phenol hydrogen-bonded as well as (5.14 Å) Pi-Pi T-shaped bonded to the center of the benzene ring and finally TRP-231 (5.90 Å) are examples of Pi-Pi T-shaped bonds attached to the center of the benzene ring. Other interactions are as in Figure 8.

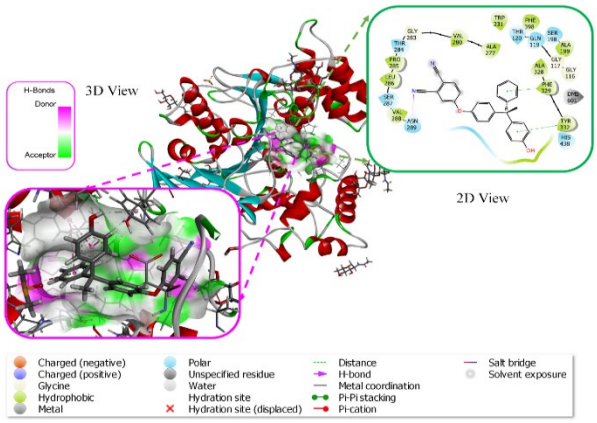

Figure 8. 3D view of hydrogen bond donor/acceptor surface on the receptor and 2D view of PN-BChE enzyme interactions.

DOI: http://dx.doi.org/10.32571/ijct.1004065 E-ISSN: 2602-277X

Figure 9 shows the 3D and 2D interaction as a result of the PN-α-GLY docking study. The affinity score for binding affinity with PN-α-GLY was calculated as -5.209 kcal/mol. Here, the bonding mechanism is conventional Hydrogen Bonding HIS-112 (2.30 Å), GLN-182 (2.34 Å) bonded to nitrogen of phthalonitrile, and hydrogen-bonded to TYR-158 (2.35 Å) phenol. ASN-415 (2.37 Å) hydrogen-bonded incompatible donor-donor bond to phenol, ASP-215 (4.39 Å) and GLU-277 (4.72 Å) Pi-anion bonded to the center of the benzene ring, TYR-158 (4.52 Å) Pi-Pi T-shaped bond attached to the center of the benzene ring, PHE-178 (4.92 Å) Pi-Pi stacking connected to the center of the benzene ring, ARG-315 (4.04 Å) and VAL-216 (5.08 Å) Pi-alkyl bond attached to the center of the benzene ring, PHE-303 (5.28 Å) and HIS-280 (5.35 Å) are examples of Pi-alkyl bond attached to the methyl group and other interactions are as in Figure 9.

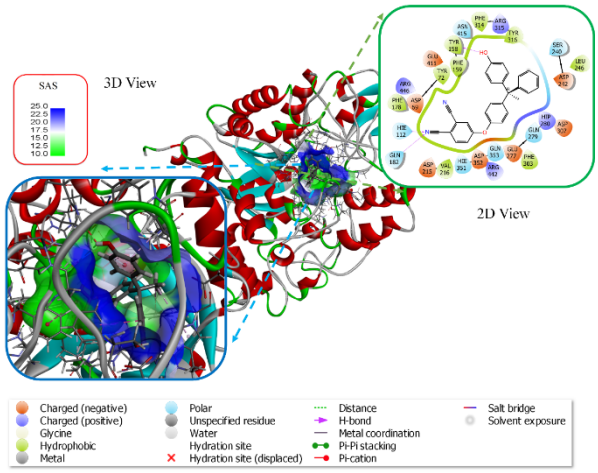

Figure 9. 3D view of the SAS surface on the receptor and 2D view of PN-α-GLY enzyme interactions.

4. CONCLUSIONS

As a result, there was one caveat that users of docking software should constantly remind themselves: their embedded models should be analyzed with a skeptical eye. In the theoretical studies and findings section, the molecule of the phthalonitrile group was first drawn in ChemBioDraw for DFT calculations in the Gaussian 09 program and minimized by the SYBL2 (mol2) method with the Chem3D program. Minimized molecules were given to the Gaussian 09 program and TD-DFT calculations (Geometry optimization, HOMO-LUMO, dipole moment calculations, MEPS maps, Mulliken atomic charges, and NBO analysis) were made for the structure. In addition, in this section, ADME analysis was performed for the compound belonging to the phthalonitrile group, and the color regions were presented separately. Among all values, PN was found to have good permeability. Finally, molecular docking studies were carried out for PN with three different enzymes (AChE, BChE, α-GLY) and docking scores and receptor models were presented. Although AChE and BChE docking scores are the highest, they have very close values.

Conflict of interests

Authors declare that there is no a conflict of interest with any person, institute, company, etc.

REFERENCES

1. Derradji, M.; Ramdani, N.; Zhang, T; Wang, J.; Gong, L-d.; Xu, X-d.; Lin, Z-w;. Henniche, A.; Rahoma, H.K.S.; Liu. W-b *Prog. Org. Coat.* **2016**, 90, 34-43.

2. Dominguez, D.D.; Keller, T.M. *Polymer.* **2007**, 48, 91-97.

3. Keller, T.M. *J Polym. Sci. A Polym. Chem.* **1988**, 26, 3199-3212.

4. Tomoda, H.; Saito, S.; Ogawa, S.; Shiraishi, S. *Chem. Lett.* **1980**, 9, 1277-1280.

5. Derradji, M.; Wang, J.; Liu, W. *In Phthalonitrile Resins and Composites*, Eds.: William Andrew Publishing, 2018, pp 107-174.

6. Derradji, M.; Wang, J.; Liu, W. *In Phthalonitrile Resins and Composites*, Eds.: William Andrew Publishing, 2018, pp 175-239.

7. Sastri, S..B.; Keller, T.M. *J Polym. Sci. A Polym. Chem.* **1998**, 36, 1885-1890.

8. Keller, T.M.; Dominguez, D.D. *Polymer.* **2005**, 46, 4614-4618.

9. Brunovska, Z.; Ishida, H. *J. Appl. Polym. Sci.* **1999**, 73, 2937-2949.

10. Hardin, C.; Pogorelov, T.V.; Luthey-Schulten, Z. *Curr. Opin. Struct. Biol.* **2002**, 12, 176-181.

11. Warzel, M.L.; Keller, T.M. *Polymer.* **1993**, 34, 663-666.

12. Brémond, É.A.G.; Kieffer, J.; Adamo, C. *J. Mol. Struct. THEOCHEM.* **2010**, 954, 52-56.

13. Guillaumont, D.; Nakamura, S. *Dyes. Pigm.* **2000**, 46, 85-92.

14. Gilad, Y;. Senderowitz, H. *J. Chem. Inf. Model.* **2014**, 54, 96-107.

15. Ekins, S.; Waller, C.L.; Swaan, PW.; Cruciani, G.; Wrighton, S.A.; Wikel, J.H. *J. Pharmacol. Tox. Met.* **2000**, 44, 251-272.

DOI: http://dx.doi.org/10.32571/ijct.1004065 **E-ISSN: 2602-277X**

16. Kaya, E.D.; Türkhan, A.; Gür, F.; Gür, B. *J. Biomol. Struct. Dyn.* **2021**, 1-14.

17. Yıldıko, Ü.; Ata, A. Ç.; Tanriverdi, A. A.; Çakmak, İ. *Bull. Mater. Sci.* **2021**, 44, 186.

18. Ağırtaş, M.S.; Cabir, B; Yıldıko, Ü.; Özdemir, S.; Gonca, S. *Chem. Pap.* **2021**, 75, 1749-1760.

19. Güngördü, Solğun, D.; Yıldıko, Ü.; Özkartal, A.; Ağırtaş, M.S. *Chem. Pap.* **2021**,

20. Bhuvaneswari, R.; Bharathi, MD.; Anbalagan, G.; Chakkaravarthi, G.; Murugesan, K.S. *J. Mol. Struct.* **2018**, 1173, 188-195.

21. Vanasundari, K.; Balachandran, V.; Kavimani, M.; Narayana, B. *J. Mol. Struct.* **2017**, 1147, 136-147.

22. Tuntland, T.; Ethell, B.; Kosaka, T.; Blasco, F.; Zang, RX.; Jain, M.; Gould, T.; Hoffmaster, K. *Front. Pharmacol.* **2014**, 5, 174.

23. Adiguzel, R.; Türkan, F.; Yildiko, Ü.; Aras, A.; Evren, E.; Onkol, T. *J. Mol. Struct.* **2021**, 1231, 129943.

24. Aras, A.; Türkan, F.; Yildiko, U.; Atalar, M.N.; Kılıç, Ö.; Alma, M.H.; Bursal, E. *Chem. Pap.* **2021**, 75, 1133-1146.